

Research Article

Crosstalk between Mitochondrial Ca^{2+} Uptake and Autophagy in Skeletal Muscle

Gaia Gherardi, Giulia Di Marco, Rosario Rizzuto , and Cristina Mammucari 

Department of Biomedical Sciences, University of Padova, 35131 Padova, Italy

Correspondence should be addressed to Cristina Mammucari; cristina.mammucari@unipd.it

Received 25 June 2019; Revised 1 August 2019; Accepted 16 August 2019; Published 8 September 2019

Guest Editor: Ulrike Hendgen-Cotta

Copyright © 2019 Gaia Gherardi et al. This is an open access article distributed under the Creative Commons Attribution License, which permits unrestricted use, distribution, and reproduction in any medium, provided the original work is properly cited.

Autophagy is responsible for the maintenance of skeletal muscle homeostasis, thanks to the removal of aberrant and dysfunctional macromolecules and organelles. During fasting, increased autophagy ensures the maintenance of the amino acid pool required for energy production. The activity of the mitochondrial Ca^{2+} uniporter (MCU), the highly selective channel responsible for mitochondrial Ca^{2+} uptake, controls skeletal muscle size, force, and nutrient utilization. Thus, both autophagy and mitochondrial Ca^{2+} accumulation play a pivotal role to maintain muscle homeostasis and to sustain muscle function. Here, we address whether, in skeletal muscle, mitochondrial Ca^{2+} uptake and autophagy are mutually related. Muscle-restricted MCU silencing partially inhibits the autophagy flux. Moreover, skeletal muscle-specific deletion of the essential autophagy gene *Atg7*, known to cause the accumulation of dysfunctional mitochondria, drastically reduces mitochondrial Ca^{2+} accumulation. Thus, a vicious cycle takes place, in which reduced MCU activity hampers the autophagic flux, and loss of autophagy further impairs mitochondrial Ca^{2+} signaling.

1. Introduction

Macroautophagy, hereafter referred to as autophagy, is a well-established mechanism responsible of the bulk degradation of intracellular macromolecules and organelles [1]. During starvation, autophagy contributes to the supplying of cellular nutrients, in particular amino acids, required for cell survival. In addition, basal autophagy, i.e., the constitutive autophagic degradation process that occurs in physiological conditions, is responsible for the degradation of dysfunctional and damaged proteins and organelles, thus ensuring the maintenance of tissue homeostasis [2].

Skeletal muscle accounts for about 40% of the total body mass, representing the main body protein pool. Muscle autophagy is induced by fasting [3, 4], and in catabolic conditions, skeletal muscle-derived amino acids are utilized as energy source by different organs [5]. In addition, as postmitotic tissue, maintenance of skeletal muscle homeostasis requires the continuous removal of aberrant macromolecules and organelles even in fed conditions. Accordingly, deletion of *Atg7*, an essential autophagy gene [6], causes muscle atrophy and accumulation of protein aggregates

and aberrant mitochondria [7]. In particular, mitochondria of skeletal muscle-specific *ATG7^{-/-}* mice are characterized by defective respiration, increased reactive oxygen species production [8], and altered membrane potential [9, 10]. The latter observation is particularly relevant in light of the fact that autophagy is modulated in response to the mitochondrial energy status [11–13]. Moreover, mitochondria are elongated in response to fasting, thus increasing the activity of the ATP synthase, ensuring physiological levels of ATP production [14].

Ca^{2+} -dependent processes occur both in the cytosol and within mitochondria. In particular, mitochondrial Ca^{2+} uptake regulates a number of cell functions, ranging from the buffering of cytosolic Ca^{2+} increases, thus indirectly regulating cytosolic Ca^{2+} -dependent processes, to intraorganelle processes, including the control of cell death [15]. In physiological conditions, mitochondrial Ca^{2+} uptake positively regulates three key dehydrogenases of the TCA cycle eventually leading to increased ATP production, thus playing a pivotal role in the control of the cellular energy status [16].

The mitochondrial Ca^{2+} uniporter (MCU), the highly selective Ca^{2+} channel located in the inner mitochondrial

membrane (IMM), is responsible for mitochondrial Ca^{2+} uptake [17, 18]. In skeletal muscle, MCU overexpression positively regulates muscle size and protects from denervation-induced loss of muscle mass [19]. This is associated with increased activity of well-known hypertrophic signaling routes, like the Akt pathway, previously reported to play an inhibitory role on autophagy [3] and to the reduced activity of the protein synthesis inhibitor and autophagy activator, GSK3 β [20, 21]. In parallel, the cell volume occupied by mitochondria is increased [19]. On the other hand, reduced or absent MCU expression, specifically in skeletal muscle, decreases muscle size, impairs muscle function, determines a slow to fast switch in MHC expression, and as a consequence of decreased PDH activity, triggers a metabolic rewiring towards preferential fatty acid utilization to counteract the reduced glucose oxidation [19, 22]. In addition, MCU silencing determines the accumulation of altered mitochondria and an overall reduction of the volume occupied by these organelles [19]. The metabolic rewiring occurring in MCU-depleted skeletal muscle eventually translates into a systemic catabolic response [22].

Ca^{2+} -dependent regulation of autophagy has been observed in a wide variety of conditions; however, whether cytosolic Ca^{2+} plays a permissive or rather an inhibitory role on autophagy induction is still debated and possibly depends on the cell type and context [23]. Moreover, increased cytosolic Ca^{2+} levels, in response to ER Ca^{2+} -depleting stimuli, induce mitochondrial Ca^{2+} accumulation that partially contributes to autophagy modulation. In particular, Cárdenas et al. reported that constitutively low levels of ER-mitochondria Ca^{2+} transfer are essential for autophagy suppression. In detail, cells lacking all three inositol 1,4,5-triphosphate receptor (InsP3R) isoforms are characterized by increased autophagy levels, that are required for cell survival during nutrient deprivation, and pharmacological inhibition of the mitochondrial Ca^{2+} uniporter phenocopies InsP3R inhibition [24]. In addition, in a genetic model of mitochondrial disorder due to a point mutation in the ND5 complex I subunit, a decrease in mitochondrial Ca^{2+} uptake is associated with an increase in the catabolic response and in the induction of pro-survival autophagy. Moreover, in patient fibroblasts, MCU overexpression restores normal levels of autophagy [25]. However, the negative modulation of mitochondrial Ca^{2+} uptake and of mitochondrial membrane potential by protein kinase C beta (PKC β) activation leads to autophagy inhibition, as opposite to starvation [26].

Thus, while the role of mitochondrial metabolism in the modulation of autophagy is undoubted, whether mitochondrial Ca^{2+} uptake increases or reduces autophagy depends, at least partially, on the cell context. Despite the significant work made to uncover the crosstalk between autophagy and mitochondrial Ca^{2+} accumulation, little is known on the role of mitochondrial Ca^{2+} uptake in the regulation of skeletal muscle autophagy. In addition, whether autophagy affects mitochondrial Ca^{2+} uptake in skeletal muscle is still obscure.

Here, we demonstrate that skeletal muscle autophagy is unaffected by MCU overexpression, while it is partially impaired by decreased MCU expression. In addition,

mitochondrial Ca^{2+} uptake is significantly reduced in autophagy-deficient skeletal muscles, thus contributing to muscle dysfunction.

2. Materials and Methods

2.1. Animals. All animal experiments were approved and performed in accordance with the Italian law D. L.vo n_26/2014. CD1 mice were purchased by Charles River Laboratories. Skeletal muscle-specific MCU knockout (skMCU $^{-/-}$) mice and their relative controls (MCU $^{fl/fl}$) were previously described [22]. Skeletal muscle-specific Atg7 knockout (skATG7 $^{-/-}$) mice and their relative controls (ATG7 $^{fl/fl}$) were previously described [7].

2.2. AAV Infection. AAV9-MCU and AAV9-shMCU were purchased from Vector Biolabs (Malvern, PA) and were previously described [19]. EDL muscles of adult CD1 mice were isolated through a small hindlimb incision, and 10^{10} vg were injected along the muscle length. Muscles were analyzed 14 days postinjection.

2.3. Autophagic Flux Measurements. Colchicine treatment: autophagic flux analyses using colchicine treatment were performed as previously described [27] with some modifications. Adult EDL muscles were injected with AAV9-MCU or AAV9-shMCU. 14 days postinfection, 0.1 mg/kg colchicine (Sigma-Aldrich) was i.p injected. Control mice received an equal volume of 0.9% NaCl. The same treatment was repeated 12 hours later. Mice were sacrificed 24 hours after the first injection; EDL muscles were harvested and frozen in liquid nitrogen-cooled isopentane. In the case of the starving mouse group, food was withdrawn at the same time of the first colchicine injection.

Leupeptin treatment: autophagic flux analyses using leupeptin treatment were performed as previously described [28] with some modifications. Adult EDL muscles were injected with AAV9-MCU or AAV9-shMCU. 14 days postinfection, 30 mg/kg leupeptin (Sigma-Aldrich) was i.p injected. Control mice received an equal volume of 0.9% NaCl. Mice were sacrificed 5 hours after the injection; EDL muscles were harvested and frozen in liquid nitrogen-cooled isopentane. In the case of the starving mouse group, food was withdrawn at the same time of the leupeptin injection.

2.4. In Vivo DNA Transfection of Mouse Skeletal Muscle. Hyaluronidase solution (2 mg/ml) (Sigma-Aldrich) was injected under the hindlimb footpads of anesthetized mice. After 30 minutes, 20 μg of plasmid DNA in 20 μl of physiological solution was similarly injected. Then, one gold-plated acupuncture needle was placed under the skin at heel, and a second one, at the base of the toes, oriented parallel to each other and perpendicular to the longitudinal axis of the foot and connected to the BTX porator (Harvard Apparatus). The muscles were electroporated by applying 20 pulses, 20 ms each, 1 s of interval to yield an electric field of 100 V. Single fiber cultures were carried out 7 days later.

2.5. Real-Time Imaging of Mitochondrial Ca^{2+} in FDB Fibers. FDB fibers were isolated 7 days after *in vivo* transfection with a plasmid encoding 4mtGCaMP6f [22]. Muscles were digested in collagenase A (4 mg/ml) (Roche) dissolved in Tyrode's salt solution (pH 7.4) (Sigma-Aldrich) containing 10% fetal bovine serum (Thermo Fisher Scientific). Single fibers were isolated, plated on laminin-coated glass coverslips, and cultured in DMEM with HEPES (42430 Thermo Fisher Scientific), supplemented with 10% fetal bovine serum, containing penicillin (100 U/ml) and streptomycin (100 μ g/ml). Fibers were maintained in culture at 37°C with 5% CO_2 .

After single fiber isolation, real-time imaging was performed. During the experiments, myofibers were maintained in Krebs-Ringer modified buffer (135 mM NaCl, 5 mM KCl, 1 mM $MgCl_2$, 20 mM HEPES, 1 mM $MgSO_4$, 0.4 mM KH_2PO_4 , 1 mM $CaCl_2$, 5.5 mM glucose, and pH 7.4) at RT, in the presence of 75 μ M N-benzyl-P-toluenesulfonamide (BTS, Tocris) to avoid the fiber contraction. 20 mM caffeine (Sigma-Aldrich) was added when indicated to elicit Ca^{2+} release from intracellular stores. Experiments were performed on a Zeiss Axiovert 200 microscope equipped with a 40 \times /1.3 N.A. Plan Fluor objective. Excitation was performed with a DeltaRAM V high-speed monochromator (Photon Technology International) equipped with a 75 W xenon arc lamp. Images were captured with a high-sensitivity Evolve 512 Delta EMCCD (Photometrics). The system is controlled by MetaMorph 7.5 (Molecular Devices) and was assembled by Crisel Instruments. 4mtGCaMP6f was alternatively excited every second at 475 and 410 nm, respectively, and images were acquired through an emission filter (535/30 nm) (Chroma). Exposure time was set to 50 ms. Acquisition was performed at binning 1 with 200 of EM gain. Image analysis was performed with Fiji distribution of the ImageJ software [29]. Images were background corrected frame by frame by subtracting the mean pixel value of a cell-free region of interest. Changes in Ca^{2+} levels (475/410 nm fluorescence ratio) were expressed as R/R_0 , where R is the ratio at time t and R_0 is the ratio at the beginning of the experiment. Mitochondrial Ca^{2+} peak was expressed as $(R-R_0)/R_0$ and normalized for the control value.

2.6. Western Blotting and Antibodies. To monitor protein levels, frozen muscles were pulverized by means of Qiagen TissueLyser and protein extracts were prepared in an appropriate buffer containing 50 mM Tris pH 7.5, 150 mM NaCl, 5 mM $MgCl_2$, 1 mM DTT, 10% glycerol, 2% SDS, 1% Triton X-100, Complete EDTA-free protease inhibitor mixture (Roche), 1 mM PMSF, 1 mM $NaVO_3$, 5 mM NaF, and 3 mM β -glycerophosphate. 40 μ g of total proteins was loaded, according to BCA quantification. Proteins were separated by SDS-PAGE electrophoresis, in commercial 4-12% acrylamide gels (Thermo Fisher Scientific), and transferred onto nitrocellulose membranes (Thermo Fisher Scientific) by semidry electrophoretic transfer. Blots were blocked for 1 hour at RT with 5% nonfat dry milk (Bio-Rad) in TBS-tween (0.5 M Tris, 1.5 M NaCl, and 0.01% Tween) solution and incubated at 4°C with primary antibodies. Secondary antibodies were incubated 1 hr at RT. The following primary

antibodies were used: anti-LC3 (1:1000, Cell Signaling), anti-p62 (1:5000, Sigma-Aldrich), anti-actin (1:20000, Santa Cruz), and anti-MCU (1:1000 Sigma-Aldrich). Secondary HRP-conjugated antibodies were purchased from Bio-Rad and used at 1:5000 dilution.

2.7. RNA Extraction, Reverse Transcription, and Quantitative Real-Time PCR. Total RNA was extracted from tibialis anterior (TA) muscles using the SV Total RNA Isolation Kit (Promega) following the manufacturer's instructions. The RNA was quantified with NanoDrop (Thermo Fisher Scientific). Complementary DNA was generated from 500 nmol of total RNA with a cDNA Synthesis Kit SuperScript II (Thermo Fisher Scientific). Oligo(dT)12–18 primers (Thermo Fisher Scientific) were used as primer for first-strand cDNA synthesis with reverse transcriptase. The obtained cDNA was analyzed by real-time PCR using the IQ5 thermocycler and the SYBR green chemistry (Bio-Rad). The primers were designed and analyzed with Primer3 [30]. The housekeeping gene Gapdh was used as an internal control for cDNA normalization. For quantification, expression levels were calculated by the Δ Ct method. Real-time PCR primer sequences were as follows: Lc3: Fw 5'-CACTGC TCTGTCTTGTGTAGGTTG-3', Rv 5'-TCGTTGTGCCT TTATTAGTGCATC-3'; Gapdh: Fw 5'-CACCATCTTCC AGGAGCGAG-3', Rv 5'-CCTTCTCCATGGTGGTGAA GAC-3'; and p62: Fw 5'-CCCAGTGTCTTGGCATTCT T-3', Rv 5'-AGGGAAAGCAGAGGAAGCTC-3'.

2.8. Statistical Analysis of Data. Statistical data are presented as mean \pm SD. Significance was calculated by Student's *t*-test or the Mann-Whitney rank sum test.

3. Results

3.1. MCU Silencing Negatively Affects Autophagy Flux in Skeletal Muscle. Muscle autophagy is induced during starvation [3], a condition characterized by a high rate of catabolism [31]. Previous work highlighted the link between mitochondrial Ca^{2+} accumulation and optimal cellular bioenergetics maintenance, demonstrating that reduced ER-mitochondrial Ca^{2+} transfer increases prosurvival autophagy in conditions of nutrient deprivation [24]. We have previously demonstrated that diminished mitochondrial Ca^{2+} uptake in skeletal muscle inhibits anabolic pathways and triggers atrophy [19]. In addition, muscle-specific MCU deletion impairs substrate oxidation and mitochondrial respiration [22]. These data suggest that, in skeletal muscle, MCU silencing could trigger autophagy induction. However, in MCU-silenced mice, the number and size of mitochondria are reduced and the frequency of severely damaged organelles is increased [19]. Since basal autophagy contributes to the removal of dysfunctional organelles and proteins [7, 32], one alternative possibility would be that MCU silencing actually negatively affects skeletal muscle autophagy.

To discern among these alternatives, we directly measured autophagy in MCU-silenced EDL muscles. We took advantage of the adenoassociated virus- (AAV-) based transduction of shMCU to specifically reduce mitochondrial Ca^{2+}

uptake in the skeletal muscle in vivo, as previously reported [19]. We monitored the lipidation of LC3 and the protein levels of p62, two well-known autophagy markers. The lipidated form of LC3, LC3-II, is embedded in the autophagosome membrane, and its levels are proportional to the number of autophagosome. p62 delivers polyubiquitinated cargoes to autophagy and accumulates in autophagy-deficient cells [33].

In MCU-silenced muscles of fed mice, LC3-II levels tend to increase compared to control muscles infected with AAV-LacZ (Figures 1(a), 1(b), 1(d), and 1(e)). This could be due either to increased autophagosome production or to increased accumulation of autophagosomes because of impaired fusion with lysosomes and/or degradation of autophagolysosomes. To distinguish between these two possibilities, we performed an analysis of the autophagic flux, i.e., the balance between formation and degradation of autophagosomes. Accordingly, we compared autophagy in muscles treated or not with either colchicine or leupeptin that causes the accumulation of autophagosomes. In detail, colchicine is a microtubule-depolymerizing agent that blocks the fusion of autophagosomes with lysosomes; instead, leupeptin is a lysosomal protease inhibitor. Thus, the LC3-II levels in leupeptin and colchicine-treated muscles represent the maximal accumulation of nondigested autophagosomes [33].

In the AAV-shLUC-infected muscles in fed condition, we observed an increase in LC3-II protein levels in colchicine- or leupeptin-treated muscles, due to the block of autophagy, as expected. AAV-shMCU-treated muscles reached maximal LC3-II levels even in the absence of inhibitor treatment (Figures 1(a), 1(b), 1(d), and 1(e)). Thus, MCU silencing triggers a block in the autophagy flux which may account for the increased number of damaged mitochondria in MCU-silenced muscles [19]. As a second marker of autophagy flux, we monitor the p62 protein levels, which accumulate in response to defective autophagy [34]. Besides autophagy-dependent degradation, p62 protein levels depend on multiple factors, including gene transcription and proteasome activity. In addition, previous observations indicate that accumulation of p62 occurs in a shifted timeframe compared to LC3-II production [33]. In our experiments, autophagy flux inhibition did not affect p62 levels in fed conditions (Figures 1(a), 1(c), 1(d), and 1(f); 2(a), 2(c), 2(d), and 2(f); and 3(a) and 3(c)) indicating that p62 does not represent here an optimal autophagic marker.

Next, we evaluated the effects of MCU silencing on the autophagic flux in conditions of nutrient deprivation and thus of energy stress. For this purpose, we measured autophagy flux in muscles of fasting animals. Fasting and treatment with autophagy inhibitors were coincident, i.e., 5 hours for leupeptin-treated muscles and 24 hours for colchicine-treated muscles. Both 5 hours and 24 hours of starvation increased LC3-II and p62 protein levels (Figure S1). MCU silencing caused a tendency towards increased LC3-II protein levels in muscles of mice deprived of food for 5 hours (Figures 1(g) and 1(h)), which became significant when starvation was prolonged to 24 hours (Figures 1(j) and 1(k)). When fasting mice

infected with AAV-shMCU in skeletal muscle were treated with leupeptin, we observed no difference in LC3-II protein levels compared to untreated shMCU-injected muscles, indicating that MCU silencing in muscles of mice fasted for 5 hours triggers a block of autophagy (Figures 1(g) and 1(h)). p62 protein levels were increased in both AAV-shLUC- and AAV-shMCU-infected muscles upon 5 hours of fasting and treatment with leupeptin (Figures 1(g)–1(i)). These data suggest that increased autophagosome production by fasting, associated with short-term treatment with an autophagy flux inhibitor, is the ideal setting to uncover p62 accumulation in skeletal muscle, at least in our experimental conditions. However, p62 protein levels were unaffected by MCU silencing (Figures 1(g)–1(i)). When mice were fasted for 24 hours and treated with colchicine, MCU-silenced muscles were autophagy-competent (Figures 1(j) and 1(k)), suggesting that prolonged starvation removes the block in autophagy caused by the reduction in mitochondrial Ca^{2+} uptake. Moreover, in muscles of mice treated with colchicine and starved for 24 hours, p62 protein levels were unaffected, again indicating the complexity of p62 homeostasis (Figures 1(j)–1(l)).

3.2. Autophagy Flux Is Functional in Skeletal Muscle-Specific MCU KO. The previous experiments demonstrate that MCU silencing partially inhibits the autophagic flux in skeletal muscle. We further investigated the modulation of autophagy in the skeletal muscle-specific MCU KO mouse (hereafter referred to as skMCU^{-/-}) in which a completed ablation of mitochondrial Ca^{2+} accumulation occurs [22]. Reduced respiration and a metabolic rewiring that comprises a catabolic systemic response characterize this mouse model.

We performed autophagy flux measurements in skMCU^{-/-} muscles both in basal and in starving conditions. In muscles of fed mice, LC3-II levels were similar in controls and in skMCU^{-/-} muscles (Figures 2(a), 2(b), 2(d), and 2(e)). When muscles were treated with the autophagy inhibitors, LC3-II levels tend to increase both in MCU^{fl/fl} and in skMCU^{-/-} muscles. However, as reported above (Figure 1), p62 levels were not affected by treatment with colchicine or leupeptin (Figures 2(a), 2(c), 2(d), and 2(f)). Then, we measured autophagy flux in muscles of fasting animals. LC3-II protein levels were similar in skMCU^{-/-} muscles compared to controls. In addition, LC3-II protein levels were increased in MCU^{fl/fl} muscles treated with leupeptin or colchicine, as expected, as well as in skMCU^{-/-} muscles (Figures 2(g), 2(h), 2(j), and 2(k)). p62 protein levels were increased by fasting associated with either leupeptin or colchicine treatment, both in MCU^{fl/fl} and in skMCU^{-/-} muscles (Figures 2(g)–2(i) and 2(j)–2(l)). To determine whether LC3-II and p62 transcription was regulated, we measured the relative mRNA levels of these two transcripts in skMCU^{-/-} muscles treated with the autophagy flux inhibitors. As reported in Figure S2, leupeptin or colchicine treatment did not increase LC3 or p62 expression, either in fed or in starved conditions, indicating that the increases in protein levels are not due to a transcriptional activation.

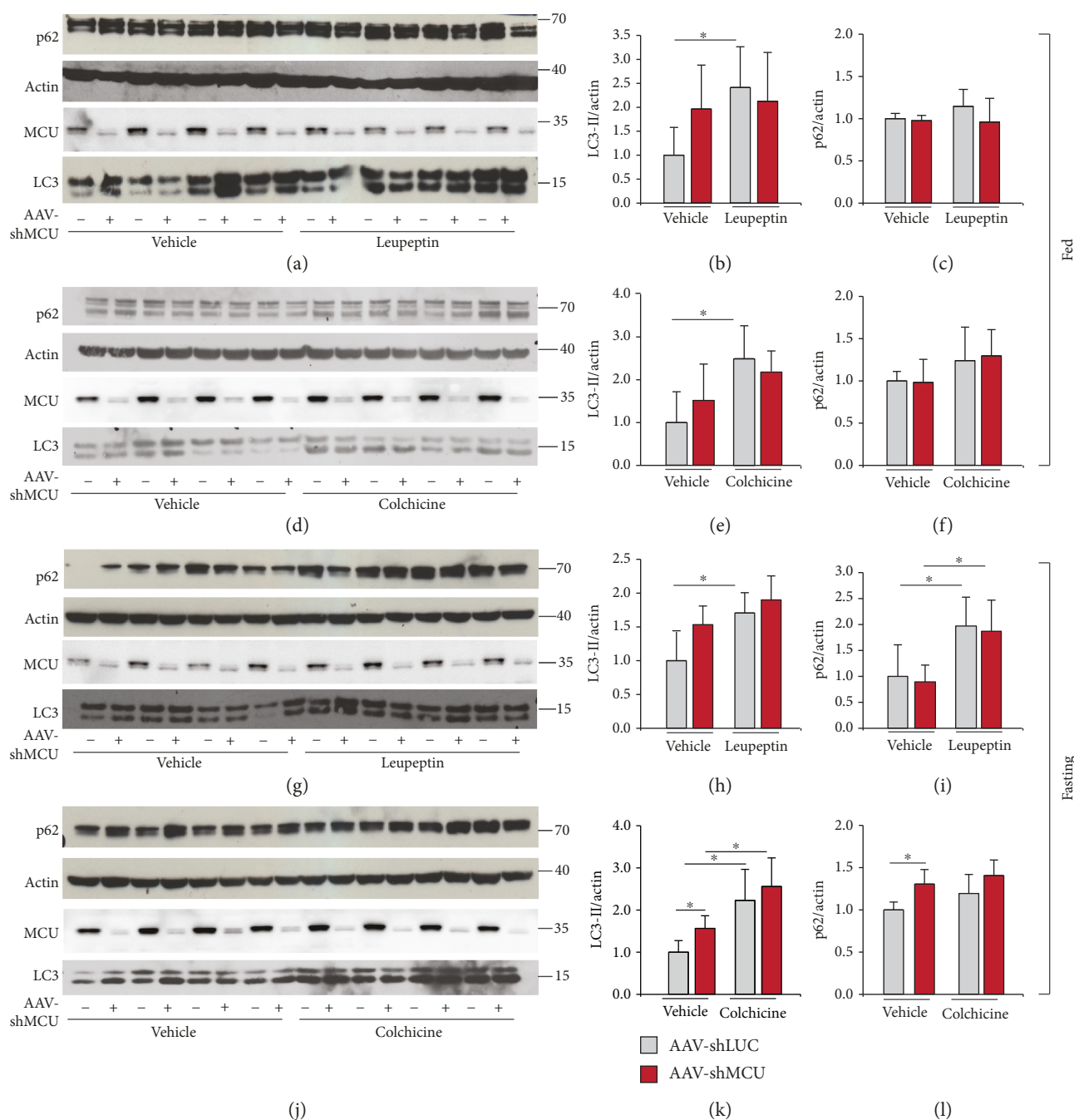


FIGURE 1: Autophagy flux analyses in MCU-silenced muscles. (a-f) Immunoblotting analysis of EDL muscles infected with AAV-shMCU or AAV-shLUC as control and treated or not with leupeptin (a-c) or colchicine (d-f) in fed conditions. Western blot analyses demonstrated efficient MCU downregulation in EDL muscles. Protein levels of LC3-II and p62 were used to monitor autophagy, relative to actin protein levels used as loading control. (b, c, e, and f) Quantification by densitometry of the ratio between LC3-II/actin and p62/actin. * $p < 0.05$, t test (two-tailed, unpaired) of four animals per condition. Data are presented as mean \pm SD. (g-l) Immunoblotting analysis of EDL muscles infected with AAV-shMCU or AAV-shLUC as control and treated or not with leupeptin (g-i) or colchicine (j-l) upon starvation. Western blot analyses demonstrated efficient MCU downregulation in EDL muscles. (h, i, k, and l) Quantification by densitometry of the ratio between LC3-II/actin and p62/actin. * $p < 0.05$, t test (two-tailed, unpaired) of four animals per condition. Data are presented as mean \pm SD.

These data indicate that autophagy flux is maintained despite the constitutive depletion of mitochondrial Ca^{2+} uptake.

3.3. MCU Overexpression Does Not Alter Autophagic Flux in Skeletal Muscle. Increased mitochondrial Ca^{2+} uptake trig-

gers muscle hypertrophy and protein synthesis [19]. Enhanced energy production and activation of anabolic signaling routes should in principle play an inhibitory effect on autophagy. On the other hand, PDH activity is unaffected by MCU overexpression [19], indicating that increased

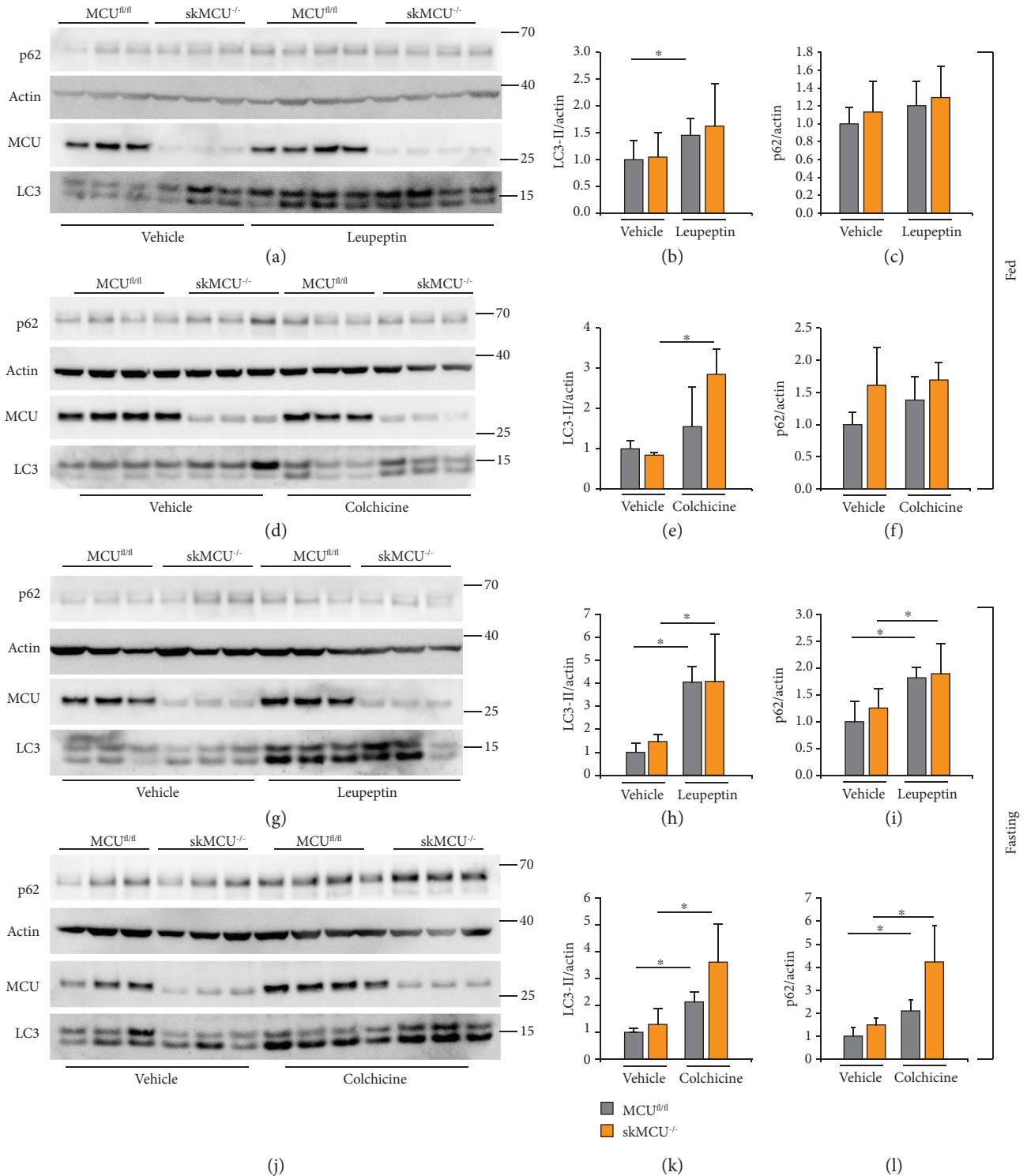


FIGURE 2: Autophagy flux analyses in *skMCU^{-/-}* mice. (a-f) Immunoblot of EDL muscles of *skMCU^{-/-}* or *skMCU^{fl/fl}* mice treated or not with leupeptin (a-c) or colchicine (d-f) in fed conditions. Western blot analyses demonstrated efficient MCU deletion in EDL muscles. LC3-II and p62 protein levels were used to monitor autophagy, relative to actin protein levels used as loading control. (b, c, e, and f) Quantification by densitometry of the ratio between LC3-II/actin and p62/actin. * $p < 0.05$, t test (two-tailed, unpaired) of three vehicle animals and four treated animals, respectively. Data are presented as mean \pm SD. (g-l) Immunoblotting analysis of EDL muscles of *skMCU^{-/-}* or *skMCU^{fl/fl}* mice treated or not with leupeptin (g-i) or colchicine (j-l) upon starvation. Western blot analyses demonstrated efficient MCU deletion in EDL muscles. (h, i, k, and l) Quantification by densitometry of the ratio between LC3-II/actin and p62/actin. * $p < 0.05$, t test (two-tailed, unpaired) of, respectively, three vehicle animals and four treated animals. Data are presented as mean \pm SD.

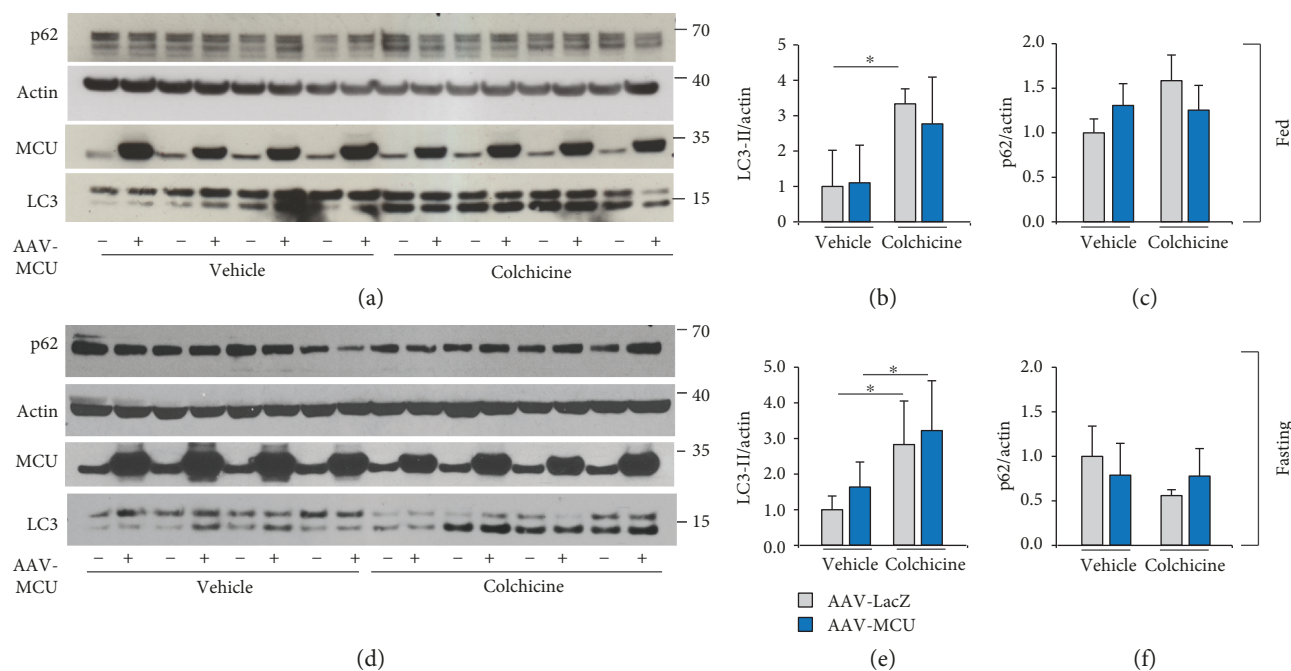


FIGURE 3: Autophagy flux analyses in MCU overexpressing muscles. (a-c) Immunoblotting analysis of EDL muscles infected with AAV-MCU or AAV-LacZ as control and treated or not with colchicine in fed conditions. Western blot analyses demonstrated efficient MCU overexpression in EDL muscles. Protein levels of LC3-II and p62 were used to monitor autophagy, relative to actin protein levels used as loading control. (b, c) Quantification by densitometry of the ratio between LC3-II/actin and p62/actin. $*p < 0.05$, t test (two-tailed, unpaired) of, respectively, three vehicle animals and four treated animals. Data are presented as mean \pm SD. (d-f) Immunoblotting analysis of EDL muscles infected with AAV-MCU or AAV-LacZ as control and treated or not with colchicine upon starvation. Western blot analyses demonstrated efficient MCU overexpression in EDL muscles. (e, f) Quantification by densitometry of the ratio between LC3-II/actin and p62/actin. $*p < 0.05$, t test (two-tailed, unpaired) of four animals per condition. Data are presented as mean \pm SD.

mitochondrial Ca^{2+} uptake does not impinge on the oxidative metabolism of muscle mitochondria.

We wondered whether the overexpression of MCU in skeletal muscle could modify either basal or induced autophagy flux. We performed autophagic flux analyses in AAV-MCU-injected muscles in fed and starving conditions. In fed animals, no difference was observed in LC3-II protein levels in MCU overexpressing muscles compared to AAV-LacZ-infected control muscles (Figures 3(a) and 3(b)), and an increase in LC3 II protein levels was observed both in mock infected and in MCU overexpressing muscles treated with colchicine (Figures 3(a) and 3(b)). In addition, p62 protein levels were unaffected by MCU overexpression (Figures 3(a) and 3(c)). These data demonstrate that MCU overexpressing muscles are autophagy-competent, not differently from control muscles, and that an increase in mitochondrial Ca^{2+} uptake does not alter the autophagy flux in fed conditions. Next, we measured whether MCU overexpression impinges on the autophagy process during starvation. We detected no difference in the LC3-II protein levels in starved muscles upon AAV-MCU infection compared to AAV-LacZ-infected muscles. In addition, we observed an increase in LC3-II protein levels in the muscles treated with colchicine, both infected with AAV-LacZ and infected with AAV-MCU (Figures 3(d) and 3(e)). Similarly to fed muscles, p62 was unaffected by MCU overexpression in fasting conditions (Figures 3(d) and 3(f)). Taken together, these results

show that MCU overexpression does not affect autophagy in skeletal muscle.

3.4. Lack of Skeletal Muscle Autophagy Causes a Decrease in Mitochondrial Ca^{2+} Uptake. It is clearly established that the deletion of the autophagy genes *Atg7* or *Atg5* in different tissues, including skeletal muscle, liver, and heart, results in swollen and aberrant mitochondria [6–8, 35]. In particular, autophagy-deficient muscles are atrophic and accumulate protein aggregates and dysfunctional mitochondria [7, 8], characterized by a decreased oxygen consumption rate and increased levels of reactive oxygen species [8]. We wondered whether these defects are associated with impaired mitochondrial Ca^{2+} signaling. For this purpose, we measured mitochondrial Ca^{2+} uptake in mice where *Atg7*, an essential gene required for autophagosome formation, is deleted specifically in skeletal muscle (hereafter referred as *skATG7^{-/-}*) [7]. We transfected in vivo the adult flexor digitorum brevis (FDB) muscles of *skATG7^{-/-}* mice with plasmids encoding a GFP-based Ca^{2+} probe targeted to mitochondria, mtGCaMP6m [22]. One week later, we performed real-time imaging experiments on isolated single myofibers. At the beginning of the experiment, we measured basal mitochondrial $[\text{Ca}^{2+}]$ and then we added caffeine to discharge the sarcoplasmic reticulum Ca^{2+} pool, driving an increase in cytosolic $[\text{Ca}^{2+}]$ and a following accumulation of Ca^{2+} into mitochondria. *skATG7^{-/-}* skeletal muscle fibers showed both

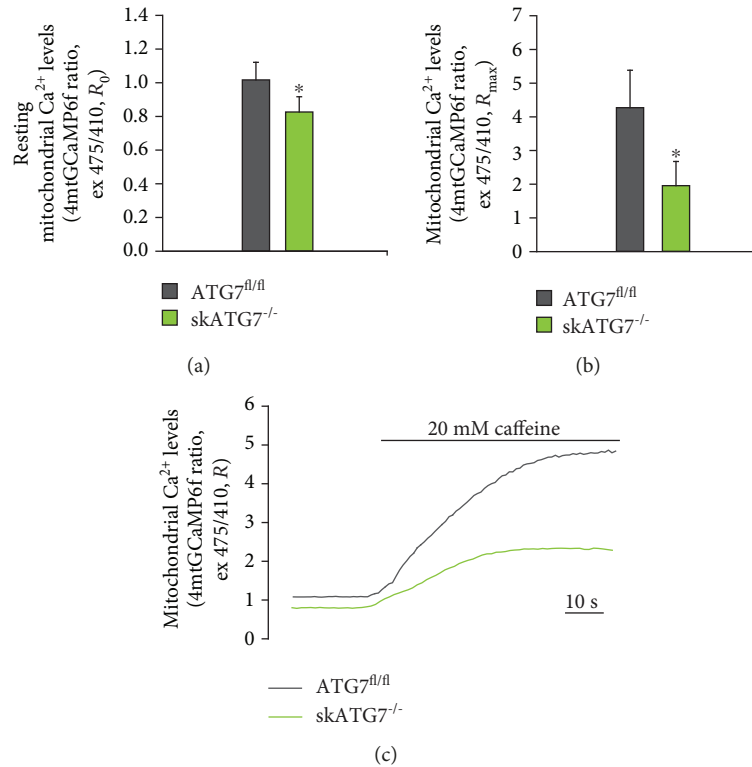


FIGURE 4: Mitochondrial Ca^{2+} uptake measurements in $\text{skATG7}^{-/-}$ mice. (a) Resting mitochondrial $[\text{Ca}^{2+}]$ was decreased in $\text{skATG7}^{-/-}$ FDB myofibers compared to $\text{ATG7}^{\text{fl/fl}}$ controls. Data are presented as mean \pm SD (>10 fibers per condition). (b) Ratiometric measurements of mitochondrial Ca^{2+} uptake upon caffeine treatment highlighted a reduction in peak mitochondrial $[\text{Ca}^{2+}]$ of $\text{skATG7}^{-/-}$ FDB myofibers compared to $\text{ATG7}^{\text{fl/fl}}$ controls. $*p < 0.05$, t test (two-tailed, unpaired) of >10 fibers per condition. Data are presented as mean \pm SD. (c) Representative traces of mitochondrial Ca^{2+} uptake measurements.

a decrease in mitochondrial Ca^{2+} uptake and a diminished resting mitochondrial $[\text{Ca}^{2+}]$ compared to $\text{ATG7}^{\text{fl/fl}}$ myofibers (Figures 4(a)–4(c)). These data suggest that loss of autophagy is associated with decreased mitochondrial Ca^{2+} uptake, either as a causal factor or as a consequence of dysfunctional mitochondria activity.

4. Discussion

A lot of effort has been made to understand how mitochondrial Ca^{2+} accumulation could regulate skeletal muscle homeostasis. $\text{MCU}^{-/-}$ mice, despite an overall mild phenotype, have significant impairment in exercise capacity and in muscle force [36]. Modulation of MCU specifically in skeletal muscle controls myofiber size impinging on anabolic signaling pathways [19, 22]. Moreover, despite decreased glucose oxidation and oxygen consumption rate [22], skeletal muscle-specific $\text{MCU}^{-/-}$ mice switch their muscle metabolism towards increased dependency on fatty acid oxidation [37] and present a systemic catabolic response which involves both liver and adipose tissue metabolic remodeling.

Mitochondrial Ca^{2+} signaling regulates autophagy; however, whether it plays a permissive or an inhibitory role depends on the different settings [11, 23]. In cells deleted of all three InsP3R isoforms, autophagy is induced as a consequence of impaired ER-mitochondria Ca^{2+} transfer that, by reducing ATP production, causes the activation of AMPK

[24]. However, in a different context, $\text{PKC}\beta$ overexpression diminishes mitochondrial Ca^{2+} uptake which eventually inhibits autophagy [26]. Finally, in fibroblasts of patients expressing a mutated subunit of the ETC complex I, mitochondrial Ca^{2+} uptake decrease is accompanied by an increase in the autophagy flux [25]. With these premises, the consequence of MCU modulation in skeletal muscle autophagy is uncertain.

Our data indicate that modulation of skeletal muscle autophagy relies on changes in mitochondrial Ca^{2+} signaling. In particular, we demonstrated that decreased MCU expression in adult animals, and thus impaired oxidative metabolism and energy production, partially hampers autophagy flux, as already suggested by Patergnani et al. [26]. However, different from $\text{PKC}\beta$ overexpressing cells, characterized by reduced mitochondrial membrane potential, this parameter is unaffected in MCU-silenced muscles [19], indicating that the mechanism underlying the inhibition of autophagy flux by MCU silencing in skeletal muscle is still unknown. In detail, in AAV-shMCU-treated muscles, autophagy flux was blocked both in fed and in fasting conditions, with one exception. When fasting was prolonged to 24 hours, in MCU-silenced muscles, autophagy flux was restored. One possibility is that prosurvival autophagy induced by starvation overcomes the inhibitory effect of MCU silencing. Importantly, the block in autophagy flux could contribute to the increased number of

aberrant mitochondria observed in AAV-shMCU muscles [19]. On the other hand, in skMCU^{-/-} muscles, autophagy flux is unaffected. This could be because long-term skeletal muscle-specific MCU deletion triggers increased muscle glucose uptake and systemic catabolic responses involving liver and adipose tissue that could in part mitigate the negative effects of reduced mitochondrial Ca²⁺ signaling on autophagy activity.

Next, we demonstrated that MCU overexpression has no effect on the autophagy flux, either in basal conditions or during starvation. One should take into account the fact that increased mitochondrial Ca²⁺ uptake plays different roles according to the cell context. For example, in the liver, mitochondrial Ca²⁺ overload triggered by MICU1 knockdown is associated with the opening of the permeability transition pore (PTP), a large-conductance channel, and eventually cell death [38]. Vice versa, in skeletal muscle, MCU overexpression does not cause any sign of myofiber damage or death [19], suggesting that healthy skeletal muscle mitochondria are prone to sustain elevated Ca²⁺ waves, without impinging on degradation processes like autophagy. Whether dysregulation of mitochondrial Ca²⁺ signaling affects mitophagy, i.e., the selective autophagic degradation of mitochondria, is an open issue and deserves further investigation.

In the second part of this work, we addressed whether impaired autophagy could alter mitochondrial Ca²⁺ uptake. We detected a decreased mitochondrial basal [Ca²⁺] and a diminished mitochondrial Ca²⁺ uptake in skeletal muscles deleted of the essential autophagy gene Atg7 [7]. This is a part of a complex scenario, in which defective mitochondria, both in terms of morphology and in terms of function, accumulate in autophagy-deficient cells and tissues [6–8, 35, 39]. This would suggest that altered mitochondrial Ca²⁺ signaling is a late consequence of the increased aberrant mitochondrial population. However, both skATG7^{-/-} and skMCU^{-/-} muscles are atrophic and have reduced oxygen consumption rates. Thus, it is plausible that reduced mitochondrial Ca²⁺ uptake in skATG7^{-/-} muscles precedes signs of mitochondrial damage and dysfunction, actively contributing to the acceleration of the degenerative process.

5. Conclusions

Skeletal muscle is characterized by great plasticity, and autophagy contributes to muscle homeostasis and response to stress stimuli. Mitochondrial Ca²⁺ signaling controls muscle trophism, activity, and metabolic adaptations. Autophagy flux is impaired by reduced mitochondrial Ca²⁺ uptake in adult skeletal muscle. Vice versa, mitochondrial Ca²⁺ signaling is decreased in autophagy-deficient myofibers, where dysfunctional organelles accumulate. However, whether this is just a consequence of the decrease number of healthy mitochondria or rather it plays a causative role is still to be determined. Possibly, a vicious cycle occurs, in which reduced mitochondrial Ca²⁺ uptake impairs the autophagy flux, and this causes the accumulation of dysfunctional mitochondria that, in turn, reduce mitochondrial Ca²⁺ signaling.

Data Availability

The data used to support the findings of this study are included within the article.

Conflicts of Interest

The authors declare that there is no conflict of interest regarding the publication of this paper.

Acknowledgments

The research was supported by fundings from the Italian Ministry of Education, University and Research (MIUR) (to CM), the AFM-Téléthon (22493 to CM), the Italian Telethon Foundation (GGP16029 to RR), and the Italian Association for Cancer Research (IG 18633 to RR). We thank Marco Sandri for the skAtg7^{-/-} mice.

Supplementary Materials

Figure S1: LC3 and p62 protein levels increase during starvation in wild type muscles, related to Figure 1. Immunoblotting analysis of wild-type EDL muscles subjected to 5 hours or 24 hours of starvation. Increases in LC3-II and p62 protein levels were detected. Actin protein levels were used as loading control. Figure S2: LC3 and p62 relative mRNA levels are modulated by leupeptin or colchicine treatment both in MCU^{fl/fl} and in skMCU^{-/-} mice, related to Figure 2. (a-d) Relative mRNA levels of LC3 and p62 in EDL muscles of skMCU^{-/-} or MCU^{fl/fl} mice treated or not with leupeptin (a-b) or colchicine (c-d) in fed conditions. **p* < 0.05, *t*-test (two-tailed, unpaired) of 3 animals per condition. Data are presented as mean ± SE. (e-h) Relative mRNA levels of LC3 and p62 in EDL muscles of skMCU^{-/-} or MCU^{fl/fl} mice treated or not with leupeptin (e-f) or colchicine (g-h) in starving conditions. **p* < 0.05, *t*-test (two-tailed, unpaired) of 3 animals per condition. Data are presented as mean ± SE. (*Supplementary Materials*)

References

- [1] N. Mizushima and D. J. Klionsky, "Protein turnover via autophagy: implications for metabolism," *Annual Review of Nutrition*, vol. 27, no. 1, pp. 19–40, 2007.
- [2] L. Galluzzi, E. H. Baehrecke, A. Ballabio et al., "Molecular definitions of autophagy and related processes," *The EMBO Journal*, vol. 36, no. 13, pp. 1811–1836, 2017.
- [3] C. Mammucari, G. Milan, V. Romanello et al., "FoxO3 controls autophagy in skeletal muscle in vivo," *Cell Metabolism*, vol. 6, no. 6, pp. 458–471, 2007.
- [4] N. Mizushima, A. Yamamoto, M. Matsui, T. Yoshimori, and Y. Ohsumi, "In vivo analysis of autophagy in response to nutrient starvation using transgenic mice expressing a fluorescent autophagosome marker," *Molecular Biology of the Cell*, vol. 15, no. 3, pp. 1101–1111, 2004.
- [5] J. M. Argilés, N. Campos, J. M. Lopez-Pedrosa, R. Rueda, and L. Rodriguez-Mañas, "Skeletal muscle regulates metabolism via interorgan crosstalk: roles in health and disease," *Journal of the American Medical Directors Association*, vol. 17, no. 9, pp. 789–796, 2016.

- [6] M. Komatsu, S. Waguri, T. Ueno et al., "Impairment of starvation-induced and constitutive autophagy in Atg7-deficient mice," *The Journal of Cell Biology*, vol. 169, no. 3, pp. 425–434, 2005.
- [7] E. Masiero, L. Agatea, C. Mammucari et al., "Autophagy is required to maintain muscle mass," *Cell Metabolism*, vol. 10, no. 6, pp. 507–515, 2009.
- [8] J. J. Wu, C. Quijano, E. Chen et al., "Mitochondrial dysfunction and oxidative stress mediate the physiological impairment induced by the disruption of autophagy," *Aging (Albany NY)*, vol. 1, no. 4, pp. 425–437, 2009.
- [9] S. Carnio, F. LoVerso, M. A. Baraibar et al., "Autophagy impairment in muscle induces neuromuscular junction degeneration and precocious aging," *Cell Reports*, vol. 8, no. 5, pp. 1509–1521, 2014.
- [10] F. Lo Verso, S. Carnio, A. Vainshtein, and M. Sandri, "Autophagy is not required to sustain exercise and PRKAA1/AMPK activity but is important to prevent mitochondrial damage during physical activity," *Autophagy*, vol. 10, no. 11, pp. 1883–1894, 2014.
- [11] K. Okamoto and N. Kondo-Okamoto, "Mitochondria and autophagy: critical interplay between the two homeostats," *Biochimica et Biophysica Acta (BBA) - General Subjects*, vol. 1820, no. 5, pp. 595–600, 2012.
- [12] F. Strappazzon, M. Vietri-Rudan, S. Campello et al., "Mitochondrial BCL-2 inhibits AMBRA1-induced autophagy," *The EMBO Journal*, vol. 30, no. 7, pp. 1195–1208, 2011.
- [13] M. Graef and J. Nunnari, "Mitochondria regulate autophagy by conserved signalling pathways," *The EMBO Journal*, vol. 30, no. 11, pp. 2101–2114, 2011.
- [14] L. C. Gomes, G. D. Benedetto, and L. Scorrano, *Nature Cell Biology*, vol. 13, no. 5, pp. 589–598, 2011.
- [15] R. Rizzuto, D. De Stefani, A. Raffaello, and C. Mammucari, "Mitochondria as sensors and regulators of calcium signalling," *Nature Reviews. Molecular Cell Biology*, vol. 13, no. 9, pp. 566–578, 2012.
- [16] C. Mammucari, G. Gherardi, and R. Rizzuto, "Structure, activity regulation, and role of the mitochondrial calcium uniporter in health and disease," *Frontiers in Oncology*, vol. 7, 2017.
- [17] D. De Stefani, A. Raffaello, E. Teardo, I. Szabò, and R. Rizzuto, "A forty-kilodalton protein of the inner membrane is the mitochondrial calcium uniporter," *Nature*, vol. 476, no. 7360, pp. 336–340, 2011.
- [18] J. M. Baughman, F. Perocchi, H. S. Girgis et al., "Integrative genomics identifies MCU as an essential component of the mitochondrial calcium uniporter," *Nature*, vol. 476, no. 7360, pp. 341–345, 2011.
- [19] C. Mammucari, G. Gherardi, I. Zamparo et al., "The mitochondrial calcium uniporter controls skeletal muscle trophism in vivo," *Cell Reports*, vol. 10, no. 8, pp. 1269–1279, 2015.
- [20] S. Schiaffino and C. Mammucari, "Regulation of skeletal muscle growth by the IGF1-Akt/PKB pathway: insights from genetic models," *Skeletal Muscle*, vol. 1, no. 1, p. 4, 2011.
- [21] N. Raben, C. Schreiner, R. Baum et al., "Suppression of autophagy permits successful enzyme replacement therapy in a lysosomal storage disorder—murine Pompe disease," *Autophagy*, vol. 6, no. 8, pp. 1078–1089, 2010.
- [22] G. Gherardi, L. Nogara, S. Ciciliot et al., "Loss of mitochondrial calcium uniporter rewires skeletal muscle metabolism and substrate preference," *Cell Death and Differentiation*, vol. 26, no. 2, pp. 362–381, 2019.
- [23] J.-P. Decuyper, G. Bultynck, and J. B. Parys, "A dual role for Ca²⁺ in autophagy regulation," *Cell Calcium*, vol. 50, no. 3, pp. 242–250, 2011.
- [24] C. Cárdenas, R. A. Miller, I. Smith et al., "Essential regulation of cell bioenergetics by constitutive InsP3 receptor Ca²⁺ transfer to mitochondria," *Cell*, vol. 142, no. 2, pp. 270–283, 2010.
- [25] V. Granatiero, V. Giorgio, T. Cali et al., "Reduced mitochondrial Ca²⁺ transients stimulate autophagy in human fibroblasts carrying the 13514A>G mutation of the ND5 subunit of NADH dehydrogenase," *Cell Death and Differentiation*, vol. 23, no. 2, pp. 231–241, 2016.
- [26] S. Patergnani, S. Marchi, A. Rimessi et al., "PRKCB/protein kinase C, beta and the mitochondrial axis as key regulators of autophagy," *Autophagy*, vol. 9, no. 9, pp. 1367–1385, 2013.
- [27] J.-S. Ju, A. S. Varadhachary, S. E. Miller, and C. C. Weihl, "Quantitation of "autophagic flux" in mature skeletal muscle," *Autophagy*, vol. 6, no. 7, pp. 929–935, 2010.
- [28] J. Haspel, R. S. Shaik, E. Ifedigbo et al., "Characterization of macroautophagic flux in vivo using a leupeptin-based assay," *Autophagy*, vol. 7, no. 6, pp. 629–642, 2011.
- [29] J. Schindelin, I. Arganda-Carreras, E. Frise et al., "Fiji: an open-source platform for biological-image analysis," *Nature Methods*, vol. 9, no. 7, pp. 676–682, 2012.
- [30] S. Rozen and H. Skaletsky, "Primer3 on the WWW for general users and for biologist programmers," in *Bioinformatics Methods and Protocols*, pp. 365–386, Humana Press, New Jersey, 2000.
- [31] M. Sandri, "Autophagy in health and disease. 3. Involvement of autophagy in muscle atrophy," *American Journal of Physiology. Cell Physiology*, vol. 298, no. 6, pp. C1291–C1297, 2010.
- [32] N. Mizushima and M. Komatsu, "Autophagy: renovation of cells and tissues," *Cell*, vol. 147, no. 4, pp. 728–741, 2011.
- [33] D. J. Klionsky, K. Abdelmohsen, A. Abe et al., "Guidelines for the use and interpretation of assays for monitoring autophagy (3rd edition)," *Autophagy*, vol. 12, no. 1, pp. 1–222, 2016.
- [34] M. Komatsu, S. Waguri, M. Koike et al., "Homeostatic levels of p62 control cytoplasmic inclusion body formation in autophagy-deficient mice," *Cell*, vol. 131, no. 6, pp. 1149–1163, 2007.
- [35] A. Nakai, O. Yamaguchi, T. Takeda et al., "The role of autophagy in cardiomyocytes in the basal state and in response to hemodynamic stress," *Nature Medicine*, vol. 13, no. 5, pp. 619–624, 2007.
- [36] X. Pan, J. Liu, T. Nguyen et al., "The physiological role of mitochondrial calcium revealed by mice lacking the mitochondrial calcium uniporter," *Nature Cell Biology*, vol. 15, no. 12, pp. 1464–1472, 2013.
- [37] J. Q. Kwong, J. Huo, M. J. Bround et al., "The mitochondrial calcium uniporter underlies metabolic fuel preference in skeletal muscle," *JCI Insight*, vol. 3, no. 22, 2018.
- [38] A. N. Antony, M. Paillard, C. Moffat et al., "MICU1 regulation of mitochondrial Ca²⁺ uptake dictates survival and tissue regeneration," *Nature Communications*, vol. 7, no. 1, 2016.
- [39] K. H. Kim, Y. T. Jeong, H. Oh et al., "Autophagy deficiency leads to protection from obesity and insulin resistance by inducing Fgf21 as a mitokine," *Nature Medicine*, vol. 19, no. 1, pp. 83–92, 2013.



Hindawi

Submit your manuscripts at
www.hindawi.com

